Few-nucleon systems in a translationally invariant harmonic oscillator basis

P. Navrátil,[1,2] G. P. Kamuntavičius,[1,3,4] and B. R. Barrett[1]
[1]*Department of Physics, University of Arizona, Tucson, Arizona 85721*
[2]*Institute of Nuclear Physics, Academy of Sciences of the Czech Republic, 250 68 Řež near Prague, Czech Republic*
[3]*Vytautas Magnus University, Kaunas LT-3000, Lithuania*
[4]*Institute of Physics, Vilnius LT-2600, Lithuania*
(Received 8 July 1999; published 9 March 2000)

We present a translationally invariant formulation of the no-core shell model approach for few-nucleon systems. We discuss a general method of antisymmetrization of the harmonic-oscillator (HO) basis depending on Jacobi coordinates. The use of a translationally invariant basis allows us to employ larger model spaces than in traditional shell-model calculations. Moreover, in addition to two-body effective interactions, three- or higher-body effective interactions as well as real three-body interactions can be utilized. In the present study we apply the formalism to solve three and four nucleon systems interacting by the CD-Bonn nucleon-nucleon (*NN*) potential in model spaces that include up to $34\hbar\Omega$ and $16\hbar\Omega$ HO excitations, respectively. Results of ground-state as well as excited-state energies, rms radii, and magnetic moments are discussed. In addition, we compare charge form factor results obtained using the CD-Bonn and Argonne V8′ *NN* potentials.

PACS number(s): 21.45.+v, 21.60.Cs, 21.30.Fe, 27.10.+h

I. INTRODUCTION

Various methods have been used to solve the few-nucleon problem in the past. The Faddeev method [1] has been successfully applied to solve the three-nucleon bound-state problem for different nucleon-nucleon potentials [2–4]. For the solution of the four-nucleon problem one can employ Yakubovsky's generalization of the Faddeev formalism [5] as done, e.g., in Refs. [6] or [7]. Alternatively, other methods have also been successfully used in the past, such as, the correlated hyperspherical harmonics expansion method [8,9] or the Green's function Monte Carlo method [10]. Apart from the coupled cluster method [11,12] applicable typically to closed-shell nuclei, the Green's function Monte Carlo method is the only approach at the present time, for which exact solutions of systems with $A>4$ interacting by realistic potentials can be obtained, with the current limit being $A=8$.

On the other hand, when studying the properties of more complex nuclei, one typically resorts to the shell model. In that approach, the single-particle harmonic-oscillator basis is used and the calculations are performed in a truncated model space. Instead of the free *NN* potential, one utilizes effective interactions appropriate for the truncated model space. Examples of such calculations are the large-basis no-core shell-model calculations that have recently been performed [13,14]. In these calculations, the effective interaction is determined for a system of two nucleons bound in a HO well and interacting by the nucleon-nucleon potential. We note that the use of a HO basis is crucial for insuring that the center-of-mass motion of the nucleus does not mix with the internal motion of the nucleons. On the one hand, this approach is limited by the model-space size, and, on the other hand, by the fact that only a two-body effective interaction is used despite the fact that higher-body effective interactions might not be negligible.

It is possible, however, to reformulate the shell-model problem in a translationally invariant way [15–17]. Recently, we combined the no-core shell-model approach to the three- and four-nucleon systems with the use of antisymmetrized translationally invariant HO basis [18,19]. That allowed us, due to the omission of the center of mass, to extend the shell-model calculations to model spaces of $32\hbar\Omega$ and $14\hbar\Omega$ excitations above the unperturbed ground state for the $A=3$ and $A=4$ systems, respectively. In addition, that approach made it possible to employ the three-body effective interactions in the $A=4$ calculations.

In the present paper we simplify and generalize this approach so that it is applicable to an arbitrary number of nucleons. In particular, we discuss in detail how to construct an antisymmetrized HO basis depending on Jacobi coordinates. We present an iterative formula for computing the antisymmetrized basis for A nucleons from the antisymmetrized basis for $A-1$ nucleons. Further, we discuss how to transform the antisymmetrized states to bases containing different antisymmetrized subclusters of nucleons.

We also describe the effective interaction derivation from a different perspective than in our previous papers. Namely, we point out the connections between the no-core shell-model approach and the unitary-model-operator approach [20]. Let us remark that a fundamental feature of the effective interactions that we employ is the fact that with the increasing model-space size the effective interactions approach the bare *NN* interaction. Therefore, in principle, our approach converges to the exact few-nucleon solution.

The basic advantage of this formalism is, first, the fact that larger model spaces can be utilized than in the standard shell-model calculations, because the center-of-mass degrees of freedom are omitted and because a coupled basis with good J and T is used. Second, due to the flexibility of HO states depending on Jacobi coordinates, different recouplings of the basis are possible. Consequently, not only can two-body effective interactions be utilized, but also three- or higher-body effective interactions as well as real three-body interactions. On the other hand, because the antisymmetrization procedure is computationally involved, the practical ap-

plicability of the formalism is limited to light nuclei. In the present formulation we expect that significant improvement over the traditional shell-model results can be achieved for $A \leqslant 6$.

We apply the formalism to solve three- and four-nucleon systems interacting by the non-local momentum-space CD-Bonn *NN* potential [21]. The present calculations are done in larger model spaces than those used in Refs. [18,19]. Also, there have not been any published results so far for the $A=4$ system interacting by the CD-Bonn *NN* potential. In addition to the calculation of ground-state and excited-state energies, point-nucleon rms radii and magnetic moments, we evaluate electromagnetic (EM) and strangeness form factors in the impulse approximation. We plan to present the results of calculations for $A=5$ and $A=6$, using the present formalism, separately.

In Sec. II, we discuss the standard no-core shell-model formulation, i.e., the Hamiltonian and effective interaction calculation. The construction of the translationally invariant HO basis is described in Sec. III. Results for $A=3$ and $A=4$ systems interacting by the CD-Bonn *NN* potential are given in Sec. IV. In Sec. V, we present concluding remarks. Technical details of evaluating matrix elements of one-, two- and three-body interactions and operators are presented in Appendixes A and B.

II. NO-CORE SHELL-MODEL APPROACH

A. Hamiltonian

In the no-core shell-model approach we start from the one- plus two-body Hamiltonian for the *A*-nucleon system, i.e.,

$$H_A = \sum_{i=1}^{A} \frac{\vec{p}_i^{\,2}}{2m} + \sum_{i<j=1}^{A} V_{\rm N}(\vec{r}_i - \vec{r}_j), \tag{1}$$

where m is the nucleon mass and $V_{\rm N}(\vec{r}_i-\vec{r}_j)$, the *NN* interaction. In order to simplify the notation, the spin and isospin dependence is omitted in the interaction term in Eq. (1). We can use both coordinate-space dependent *NN* potentials, such as the Reid, Nijmegen [22], or Argonne [10] as well as momentum-space dependent *NN* potentials, such as the CD-Bonn [21]. In the next step we modify the Hamiltonian (1) by adding to it the center-of-mass HO potential $\frac{1}{2}Am\Omega^2\vec{R}^2$, $\vec{R}=(1/A)\Sigma_{i=1}^{A}\vec{r}_i$. This potential does not influence intrinsic properties of the many-body system. It allows us, however, to work with a convenient HO basis and provides a mean field that facilitates the calculation of effective interactions. The modified Hamiltonian, depending on the HO frequency Ω, can be cast into the form

$$H_A^{\Omega} = \sum_{i=1}^{A} \left[\frac{\vec{p}_i^{\,2}}{2m} + \frac{1}{2}m\Omega^2\vec{r}_i^{\,2} \right] + \sum_{i<j=1}^{A} \left[V_{\rm N}(\vec{r}_i-\vec{r}_j) - \frac{m\Omega^2}{2A}(\vec{r}_i-\vec{r}_j)^2 \right]. \tag{2}$$

The interaction term of the Hamiltonian (2) depends only on the relative coordinates. The one-body term in Eq. (2) can be rewritten as a sum of the center-of-mass term, and a term depending on the relative coordinates.

The shell-model calculations are performed in a finite model space. Therefore, the interaction term in Eq. (2) must be replaced by an effective interaction. In general, for an *A*-nucleon system, an *A*-body effective interaction is needed. In practice, the effective interaction is usually approximated by a two-body effective interaction. In the present study we will also employ a three-body effective interaction. As approximations are involved in the effective interaction treatment, large model spaces are desirable. In that case, the calculation should be less affected by any imprecision of the effective interaction. The same is true for the evaluation of any observable characterized by an operator. In the model space, renormalized effective operators are required. The larger the model space, the less renormalization is needed.

As the Hamiltonian H_A^{Ω} (2) differs from the Hamiltonian H_A (1) only by a center-of-mass dependent term, no dependence on Ω should exist for the intrinsic properties of the nucleus. However, because of the approximations involved in the effective interaction derivation, a dependence on Ω appears in our calculations. This dependence decreases as the size of the model-space is increased.

B. Effective interaction theory in Lee-Suzuki approach

In our approach we employ the Lee-Suzuki similarity transformation method [23,24], which yields a starting-energy independent Hermitian effective interaction. In this subsection we recapitulate general formulation and basic results of this method. Applications of this method for computation of two- or three-body effective interactions are described in the following subsections.

Let us consider an *arbitrary* Hamiltonian H with the eigensystem $E_k, |k\rangle$, i.e.,

$$H|k\rangle = E_k|k\rangle. \tag{3}$$

Let us further divide the full space into the model space defined by a projector P and the complementary space defined by a projector Q, $P+Q=1$. A similarity transformation of the Hamiltonian $e^{-\omega}He^{\omega}$ can be introduced with a transformation operator ω satisfying the condition $\omega = Q\omega P$. The transformation operator is then determined from the requirement of decoupling of the Q-space and the model space as follows:

$$Qe^{-\omega}He^{\omega}P = 0. \tag{4}$$

If we denote the model space basis states as $|\alpha_P\rangle$, and those which belong to the Q-space, as $|\alpha_Q\rangle$, then the relation $Qe^{-\omega}He^{\omega}P|k\rangle = 0$, following from Eq. (4), will be satisfied for a particular eigenvector $|k\rangle$ of the Hamiltonian (3), if its *Q*-space components can be expressed as a combination of its *P*-space components with the help of the transformation operator ω, i.e.,

$$\langle \alpha_Q|k\rangle = \sum_{\alpha_P} \langle \alpha_Q|\omega|\alpha_P\rangle\langle \alpha_P|k\rangle. \tag{5}$$

If the dimension of the model space is d_P, we may choose a set $\mathcal{K}$ of d_P eigenevectors, for which the relation (5) will be satisfied. Under the condition that the $d_P \times d_P$ matrix $\langle \alpha_P|k\rangle$ for $|k\rangle \in \mathcal{K}$ is invertible, the operator ω can be determined from Eq. (5) as

$$\langle \alpha_Q|\omega|\alpha_P\rangle = \sum_{k\in\mathcal{K}} \langle \alpha_Q|k\rangle\langle \tilde{k}|\alpha_P\rangle, \tag{6}$$

where we denote by tilde the inverted matrix of $\langle \alpha_P|k\rangle$, e.g., $\Sigma_{\alpha_P}\langle \tilde{k}|\alpha_P\rangle\langle \alpha_P|k'\rangle = \delta_{k,k'}$, for $k,k' \in \mathcal{K}$.

The Hermitian effective Hamiltonian defined on the model space P is then given by [24]

$$\overline{H}_{\rm eff} = [P(1+\omega^\dagger\omega)P]^{1/2} PH(P+Q\omega P)[P(1+\omega^\dagger\omega)P]^{-1/2}. \tag{7}$$

By making use of the properties of the operator ω, the effective Hamiltonian $\overline{H}_{\rm eff}$ can be rewritten in an explicitly Hermitian form as

$$\overline{H}_{\rm eff} = [P(1+\omega^\dagger\omega)P]^{-1/2}(P+P\omega^\dagger Q)H(Q\omega P+P) \times [P(1+\omega^\dagger\omega)P]^{-1/2}. \tag{8}$$

With the help of the solution for ω (6) we obtain a simple expression for the matrix elements of the effective Hamiltonian

$$\langle \alpha_P|\overline{H}_{\rm eff}|\alpha_{P'}\rangle = \sum_{k\in\mathcal{K}} \sum_{\alpha_{P''}} \sum_{\alpha_{P'''}} \langle \alpha_P|(1+\omega^\dagger\omega)^{-1/2}|\alpha_{P''}\rangle \times \langle \alpha_{P''}|\tilde{k}\rangle E_k \langle \tilde{k}|\alpha_{P'''}\rangle \times \langle \alpha_{P'''}|(1+\omega^\dagger\omega)^{-1/2}|\alpha_{P'}\rangle. \tag{9}$$

For computation of the matrix elements of $(1+\omega^\dagger\omega)^{-1/2}$, we can use the relation

$$\langle \alpha_P|(1+\omega^\dagger\omega)|\alpha_{P''}\rangle = \sum_{k\in\mathcal{K}} \langle \alpha_P|\tilde{k}\rangle\langle \tilde{k}|\alpha_{P''}\rangle, \tag{10}$$

to remove the summation over the Q-space basis states. The effective Hamiltonian (9) reproduces the eigenenergies $E_k, k \in \mathcal{K}$ in the model space. We note that the relation (9) used together with Eq. (10) does not contain any summation over the Q-space basis and, thus, represents a simplification compared to the formulas we presented in our previous papers [14,18,19], though it is fully equivalent.

C. Unitary transformation of the Hamiltonian and the two-body effective interaction

We now return to our problem, namely, to derive the effective interaction corresponding to a chosen model space for the *particular* Hamiltonian H_A^Ω (2). Let us write the Hamiltonian (2) schematically as

$$H_A^\Omega = \sum_{i=1}^{A} h_i + \sum_{i<j=1}^{A} V_{ij}. \tag{11}$$

According to Providencia and Shakin [25], a unitary transformation of the Hamiltonian, which is able to accommodate the short-range two-body correlations in a nucleus, can be introduced by choosing a two-body anti-Hermitian operator S, such that

$$\mathcal{H} = e^{-S} H_A^\Omega e^S. \tag{12}$$

Consequently, the transformed Hamiltonian can be expanded in a cluster expansion

$$\mathcal{H} = \mathcal{H}^{(1)} + \mathcal{H}^{(2)} + \mathcal{H}^{(3)} + \cdots, \tag{13}$$

where the one-body, two-body, and three-body terms are given as

$$\mathcal{H}^{(1)} = \sum_{i=1}^{A} h_i, \tag{14a}$$

$$\mathcal{H}^{(2)} = \sum_{i<j=1}^{A} \tilde{V}_{ij}, \tag{14b}$$

$$\mathcal{H}^{(3)} = \sum_{i<j<k=1}^{A} \tilde{V}_{ijk}, \tag{14c}$$

with

$$\tilde{V}_{12} = e^{-S_{12}}(h_1+h_2+V_{12})e^{S_{12}} - (h_1+h_2), \tag{15a}$$

$$\tilde{V}_{123} = e^{-S_{123}}(h_1+h_2+h_3+V_{12}+V_{13}+V_{23})e^{S_{123}} - (h_1+h_2+h_3+\tilde{V}_{12}+\tilde{V}_{13}+\tilde{V}_{23}), \tag{15b}$$

and $S_{123} = S_{12}+S_{23}+S_{31}$. In the above equations, it has been assumed that the basis states are eigenstates of the one-body, in our case HO, Hamiltonian $\Sigma_{i=1}^{A} h_i$.

If the full space is divided into a model space and a Q-space, using the projectors P and Q with $P+Q=1$, it is possible to determine the transformation operator S_{12} from the decoupling condition

$$Q_2 e^{-S_{12}}(h_1+h_2+V_{12})e^{S_{12}}P_2 = 0, \tag{16}$$

and the simultaneous restrictions $P_2 S_{12} P_2 = Q_2 S_{12} Q_2 = 0$. Note that two-nucleon-state projectors appear in Eq. (16), whose definitions follow from the definitions of the A-nucleon projectors P, Q. This approach, introduced by Suzuki and Okamoto and referred to as the unitary-model-operator approach (UMOA) [20], has a solution that can be expressed in the following form:

$$S_{12} = \operatorname{arctanh}(\omega - \omega^\dagger), \tag{17}$$

with the operator ω satisfying $\omega = Q_2 \omega P_2$. This is the same operator that solves Eq. (4) with $H = h_1 + h_2 + V_{12}$. Moreover, $P_2 e^{-S_{12}}(h_1 + h_2 + V_{12}) e^{S_{12}} P_2$ is given by Eq. (8) with $H = h_1 + h_2 + V_{12}$.

D. Two-body effective interaction calculation

We compute the two-body effective interaction according to Eq. (15a) using the decoupling condition (16). For the two-nucleon Hamiltonian we employ

$$H_2^{\Omega} = H_{02} + V_{12} = \frac{\vec{p}^2}{2m} + \frac{1}{2} m\Omega^2 \vec{r}^2 + V_{\mathrm{N}}(\sqrt{2}\vec{r}) - \frac{m\Omega^2}{A}\vec{r}^2, \tag{18}$$

where $\vec{r} = \sqrt{\frac{1}{2}}(\vec{r}_1 - \vec{r}_2)$ and $\vec{p} = \sqrt{\frac{1}{2}}(\vec{p}_1 - \vec{p}_2)$ and where H_{02} differs from $h_1 + h_2$ by the omission of the center-of-mass HO term of nucleons 1 and 2. Our calculations start with exact solutions of the Hamiltonian (18) and, consequently, we construct the operator ω and, then, the effective interaction directly from these solutions by application of the relations (6) and (9) with $E_k, |k\rangle$ obtained from the solution of the Schrödinger equation (3) for the Hamiltonian $H = H_2^{\Omega}$. The relative-coordinate two-nucleon HO states used in the calculation are characterized by quantum numbers $|nlsjt\rangle$ with the radial and orbital HO quantum numbers corresponding to coordinate $\vec{r}$ and momentum $\vec{p}$. Typically, we solve the two-nucleon Hamiltonian (18) for all two-nucleon channels up to $j = 6$. For the channels with higher j only the kinetic-energy term is used in the many-nucleon calculation. The model space is defined by the maximal number of allowed HO excitations $N_{\max}$ from the condition $2n + l \leqslant N_{\max}$.

In order to construct the operator ω (6) we need to select the set of eigenvectors $\mathcal{K}$. In the present application we select the lowest states obtained in each channel. It turns out that these states also have the largest overlap with the model space. Their number is given by the number of basis states satisfying $2n + l \leqslant N_{\max}$.

Finally, the two-body effective interaction is determined from the two-nucleon effective Hamiltonian, obtained from Eq. (9), as $V_{2\mathrm{eff}} = \overline{H}_{2\mathrm{eff}} - H_{02}$. Apart from being a function of the nucleon number A, $V_{2\mathrm{eff}}$ depends on the HO frequency Ω and on the model-space defining parameter $N_{\max}$. It has the important property that $V_{2\mathrm{eff}} \to V_{12}$ for $N_{\max} \to \infty$ following from the fact that $\omega \to 0$ for $P \to 1$.

E. Three-body effective interaction calculation

In the standard shell-model calculations the effective interaction is limited to a two-body effective interaction. In our approach the limitation to a two-body effective interaction means that we use $V_{2\mathrm{eff}}$, computed as discussed in the previous subsection, and neglect all the three- and higher-body clusters appearing in the expansion (13). The formalism laid out in the present paper allows us, however, to employ three-body or even higher-body interactions in a straightforward manner. Therefore, we are in a position to go beyond the two-body effective interaction approximation. One way to proceed is to evaluate the three-body term appearing in Eqs. (13)–(15b). That term depends, through S_{123} in Eqs. (15a), and (15b) on the operator ω, appearing in Eq. (17), used for the construction of the two-body effective interaction. It does not, however, guarantee the model space and the Q-space decoupling for the three-nucleon system in a similar way as in Eq. (16) for the two-nucleon system. To improve on this point, we, therefore, choose a different way of deriving the three-body effective interaction. In our previous paper [19] we introduced a procedure applicable for nuclei with $A \geqslant 4$ that calculates the three-body correlations directly and guarantees the model space and Q-space decoupling for the three-nucleon system.

In order to calculate the three-body effective interaction in this way, we first rewrite the two-body interaction term of the Hamiltonian (2) and (11) using

$$\sum_{i<j=1}^{A} V_{ij} = \frac{1}{A-2} \sum_{i<j<k=1}^{A} (V_{ij} + V_{ik} + V_{jk}), \tag{19}$$

valid for $A \geqslant 3$. Then, formally, our Hamiltonian consists only of one-body and three-body terms. We now calculate the three-body effective interaction that corresponds to $V_{ij} + V_{ik} + V_{jk}$ from the three-nucleon system condition

$$Q_3 e^{-S^{(3)}}(h_1 + h_2 + h_3 + V_{12} + V_{13} + V_{23}) e^{S^{(3)}} P_3 = 0, \tag{20}$$

in complete analogy to Eq. (16). Note that $S^{(3)}$ is different from S_{123} and is determined by Eq. (20). The three-body effective interaction is then obtained utilizing the solutions of the three-nucleon system solutions from Eqs. (3), (6), and (9) for the Hamiltonian

$$H_3^{\Omega} = h_1 + h_2 + h_3 + V_{12} + V_{13} + V_{23}. \tag{21}$$

As the interaction depends only on the relative positions of nucleons 1, 2 and 3, the three-nucleon center of mass can be separated, when solving Schrödinger equation with H_3^{Ω}. Similarly as for the two-nucleon Hamiltonian (18), the center-of-mass term is not considered in the effective-interaction calculation. We obtain the three-nucleon solutions corresponding to the Hamiltonian (21) by, first, introducing Jacobi coordinates, as described later in this paper and also as described in our previous papers [18,19,26] and, by, second, the introducing for the interactions V_{12}, V_{13}, V_{23} the two-body effective interactions corresponding to a large space characterized by $N_{3\max} \approx 30$ and derived according to the procedure described in the previous subsection. A space of this size is sufficient for obtaining exact or almost exact solutions of the three-nucleon problem [18]. We note that

$$V_{ij} = V_{\mathrm{N}}(\vec{r}_i - \vec{r}_j) - \frac{m\Omega^2}{2A}(\vec{r}_i - \vec{r}_j)^2, \quad i,j = 1,2,3, \tag{22}$$

yields a three-nucleon bound system for $A \geqslant 4$. Therefore, as in the case of the two-body effective interaction calculation, the Lee-Suzuki approach is applicable, as described in Sec. II B, in a straightforward way. We use the solutions of the three-nucleon system to construct the operator ω and, then,

the three-body effective interaction directly from these solutions by applications of the relations (6) and (9). The eigensystem E_k, $|k\rangle$ is obtained from the solution of Schrödinger equation (3) for the Hamiltonian (21) with the interactions V_{ij} replaced by $V_{2\text{eff},ij}$, where the two-body effective interaction corresponds to the space defined by $N_{3\max}$, as discussed above. The model space, defined by the projector P_3, is characterized by the maximal allowed number of HO excitations $N_{\max}$, where $N_{\max}<N_{3\max}$. It is spanned by all states satisfying the condition $N_3\leqslant N_{\max}$ with N_3 given as $N_3=2n+l+2\mathcal{N}+\mathcal{L}$ when basis (29) is used, or, using the basis (32) $N_3\equiv N$. The Q-space defined by Q_3 is spanned by states with total number of HO excitations $N_{\max}<N_3\leqslant N_{3\max}$. Typically, we solve the three-nucleon system and construct the three-body effective interaction only for three-nucleon channels with $J_3=1/2^{\pm},3/2^{\pm}$ and $T_3=1/2$. For all other channels the two-body effective interaction $\Sigma_{i<j=1}^{3}V_{2\text{eff},ij}$ corresponding to the model space characterized by $N_{\max}$ is used instead.

In order to construct the operator ω (6) we need to select the set of eigenvectors $\mathcal{K}$. As in the two-body effective interaction calculation, the lowest states obtained in each channel are selected. Again, those states also have the largest overlap with the model space. Their number is given by the number of basis states with the total number of HO excitations $N_3\leqslant N_{\max}$. The three-body effective interaction is determined from the three-nucleon effective Hamiltonian, obtained from Eq. (9), as $V_{3\text{eff}}=\overline{H}_{3\text{eff}}-H_{03}$ with H_{03} equal to $h_1+h_2+h_3$ minus the three-nucleon center-of-mass HO term. Like the two-body effective interaction $V_{2\text{eff}}$, apart from being a function of the nucleon number A, $V_{3\text{eff}}$ depends on the HO frequency Ω and on the model-space defining-parameter $N_{\max}$. In addition, it also depends on the choice of $N_{3\max}$. Obviously, $N_{3\max}$ must be sufficiently large, in order to make this dependence negligible. The limiting properties of $V_{3\text{eff}}$ are as follows: $V_{3\text{eff}}\to\Sigma_{i<j=1}^{3}V_{2\text{eff},ij}$ for $N_{\max}\to N_{3\max}$ and $V_{3\text{eff}}\to\Sigma_{i<j=1}^{3}V_{ij}$ for $N_{\max},N_{3\max}\to\infty$.

III. TRANSLATIONALLY INVARIANT HARMONIC-OSCILLATOR BASIS

As discussed in the previous sections, by using the effective interaction theory we arrive at a Hamiltonian that has the following structure:

$$H_{A\text{eff}}^{\Omega}=\sum_{i=1}^{A}\left[\frac{\vec{p}_i^{\,2}}{2m}+\frac{1}{2}m\Omega^2\vec{r}_i^{\,2}\right]+\left\{\sum_{i<j=1}^{A}\left[V_{\text{N}}(\vec{r}_i-\vec{r}_j)-\frac{m\Omega^2}{2A}(\vec{r}_i-\vec{r}_j)^2\right]\right\}_{\text{eff}}, \tag{23}$$

with the interaction term depending on relative coordinates (and/or relative momenta) only. The center-of-mass dependence appears only in the one-body HO term. Consequently, by performing a transformation to Jacobi coordinates, the center-of-mass degrees of freedom can be removed.

A. Jacobi coordinates

We work in the isospin formalism and consider nucleons with the mass m. A generalization to the proton-neutron formalism with unequal masses for the proton and the neutron is straightforward. We will use Jacobi coordinates that are introduced as an orthogonal transformation of the single-nucleon coordinates. In general, Jacobi coordinates are proportional to differences of centers of mass of nucleon subclusters.

For our purposes we need three different sets of Jacobi coordinates. The first set, i.e.,

$$\vec{\xi}_0=\sqrt{\frac{1}{A}}[\vec{r}_1+\vec{r}_2+\cdots+\vec{r}_A], \tag{24a}$$

$$\vec{\xi}_1=\sqrt{\frac{1}{2}}[\vec{r}_1-\vec{r}_2], \tag{24b}$$

$$\vec{\xi}_2=\sqrt{\frac{2}{3}}\left[\frac{1}{2}(\vec{r}_1+\vec{r}_2)-\vec{r}_3\right], \tag{24c}$$

$$\cdots$$

$$\vec{\xi}_{A-2}=\sqrt{\frac{A-2}{A-1}}\left[\frac{1}{A-2}(\vec{r}_1+\vec{r}_2+\cdots+\vec{r}_{A-2})-\vec{r}_{A-1}\right], \tag{24d}$$

$$\vec{\xi}_{A-1}=\sqrt{\frac{A-1}{A}}\left[\frac{1}{A-1}(\vec{r}_1+\vec{r}_2+\cdots+\vec{r}_{A-1})-\vec{r}_A\right], \tag{24e}$$

is used for the construction of the antisymmetrized HO basis. Here, $\vec{\xi}_0$ is proportional to the center of mass of the A-nucleon system. On the other hand, $\vec{\xi}_\rho$ is proportional to the relative position of the $(\rho+1)$st nucleon and the center of mass of the ρ nucleons.

Another set that is suitable for the basis expansion, when two-body interaction matrix elements need to be calculated, is obtained by keeping $\vec{\xi}_0,\vec{\xi}_1,\ldots\vec{\xi}_{A-3}$ and introducing two different variables, as follows:

$$\vec{\xi}_0,\vec{\xi}_1,\cdots\vec{\xi}_{A-3}, \tag{25a}$$

$$\vec{\eta}_{A-2}=\sqrt{\frac{2(A-2)}{A}}\left[\frac{1}{A-2}(\vec{r}_1+\vec{r}_2+\cdots+\vec{r}_{A-2})-\frac{1}{2}(\vec{r}_{A-1}+\vec{r}_A)\right], \tag{25b}$$

$$\vec{\eta}_{A-1}=\sqrt{\frac{1}{2}}[\vec{r}_{A-1}-\vec{r}_A]. \tag{25c}$$

Eventually, a set suitable for the basis expansion, when three-body interaction matrix elements need to be calculated, is obtained by keeping $\vec{\xi}_0,\vec{\xi}_1,\ldots\vec{\xi}_{A-4}$ and $\vec{\eta}_{A-1}$ from the previous set and introducing two other different variables

$$\vec{\xi}_0, \vec{\xi}_1, \cdots \vec{\xi}_{A-4}, \tag{26a}$$

$$\vec{\vartheta}_{A-3} = \sqrt{\frac{3(A-3)}{A-2}}\left[\frac{1}{A-3}(\vec{r}_1+\vec{r}_2+\ \ldots\ +\vec{r}_{A-3}) - \frac{1}{3}(\vec{r}_{A-2}+\vec{r}_{A-1}+\vec{r}_A)\right], \tag{26b}$$

$$\vec{\vartheta}_{A-2} = \sqrt{\frac{2}{3}}\left[\frac{1}{2}(\vec{r}_{A-1}+\vec{r}_A)-\vec{r}_{A-2}\right], \tag{26c}$$

$$\vec{\eta}_{A-1} = \sqrt{\frac{1}{2}}[\vec{r}_{A-1}-\vec{r}_A]. \tag{26d}$$

Identical transformations, as in Eqs. (24a)–(26d), are also introduced for the momenta.

Let us note that the one-body HO potential in Eq. (23) transforms as

$$\sum_{i=1}^{A}\frac{1}{2}m\Omega^2\vec{r}_i^{\,2} = \frac{1}{2}m\Omega^2\vec{\xi}_0^{\,2} + \sum_{\rho=1}^{A-1}\frac{1}{2}m\Omega^2\vec{\xi}_\rho^{\,2}, \tag{27}$$

and the kinetic term transforms in an analogous way. As the interaction does not depend on $\vec{\xi}_0$ or the center-of-mass momentum, the center-of-mass HO term can be omitted. Moreover, we can use the HO basis, depending on coordinates $\vec{\xi}_\rho, \rho = 1,2 \ldots A-1$, e.g.,

$$\prod_{\rho=1}^{A-1}\langle\vec{\xi}_\rho|n_\rho l_\rho\rangle, \tag{28}$$

for our calculations. First, let us remark that due to the othogonality of the transformations (24a)–(26d), the same HO parameter is used for all HO wave functions. Second, we may use any of the sets (24a)–(26d) for the basis construction of the type (28), as similar relations like Eq. (27) hold for all the sets. Third, the basis (28) is *not* antisymmetrized with respect to the exchanges of all nucleon pairs. The antisymmetrization procedure will be discussed in the following subsections.

B. Antisymmetrization for the three-nucleon system

We discussed the antisymmetrization of the translationally invariant HO basis for the three-nucleon system in our previous papers [18,19,26]. One starts by introducing a basis following from Eq. (28) that depends on Jacobi coordinates $\vec{\xi}_1$ and $\vec{\xi}_2$, defined in Eqs. (24a)–(24e), e.g.,

$$|(nlsjt;\mathcal{NLJ})JT\rangle. \tag{29}$$

Here n,l and $\mathcal{N},\mathcal{L}$ are the HO quantum numbers corresponding to the harmonic oscillators associated with the coordinates (and the corresponding momenta) $\vec{\xi}_1$ and $\vec{\xi}_2$, respectively. The quantum numbers s,t,j describe the spin, isospin and angular momentum of the relative-coordinate two-nucleon channel of nucleons 1 and 2, while $\mathcal{J}$ is the angular momentum of the third nucleon relative to the center of mass of nucleons 1 and 2. The J and T are the total angular momentum and the total isospin, respectively. Note that the basis (29) is antisymmetrized with respect to the exchanges of nucleons 1 and 2, as the two-nucleon channel quantum numbers are restricted by the condition $(-1)^{l+s+t}=-1$. It is not, however, antisymmetrized with respect to the exchanges of nucleons $1\leftrightarrow3$ and $2\leftrightarrow3$. In order to construct a completely antisymmetrized basis, one needs to obtain eigenvectors of the antisymmetrizer

$$\mathcal{X} = \frac{1}{3}(1+\mathcal{T}^{(-)}+\mathcal{T}^{(+)}), \tag{30}$$

where $\mathcal{T}^{(+)}$ and $\mathcal{T}^{(-)}$ are the cyclic and the anticyclic permutation operators, respectively. The antisymmetrizer $\mathcal{X}$ is a projector satisfying $\mathcal{X}\mathcal{X}=\mathcal{X}$. When diagonalized in the basis (29), its eigenvectors span two eigenspaces. One, corresponding to the eigenvalue 1, is formed by physical, completely antisymmetrized states and the other, corresponding to the eigenvalue 0, is formed by spurious states. There are about twice as many spurious states as the physical ones [26].

Due to the antisymmetry with respect to the exchanges $1\leftrightarrow2$, the matrix elements in the basis (29) of the antisymmetrizer $\mathcal{X}$ can be evaluated simply as $\langle\mathcal{X}\rangle=\frac{1}{3}(1-2\langle\mathcal{T}_{23}\rangle)$, where $\mathcal{T}_{23}$ is the permutation corresponding to the exchange of nucleons 2 and 3. Its matrix element can be evaluated in a straightforward way, e.g.,

$$\begin{aligned}&\langle(n_1l_1s_1j_1t_1;\mathcal{N}_1\mathcal{L}_1\mathcal{J}_1)JT|\mathcal{T}_{23}|(n_2l_2s_2j_2t_2;\mathcal{N}_2\mathcal{L}_2\mathcal{J}_2)JT\rangle\\ &\quad=\delta_{N_1,N_2}\hat{t}_1\hat{t}_2\begin{Bmatrix}\frac{1}{2}&\frac{1}{2}&t_1\\ \frac{1}{2}&T&t_2\end{Bmatrix}\sum_{LS}\hat{L}^2\hat{S}^2\hat{j}_1\hat{j}_2\hat{\mathcal{J}}_1\hat{\mathcal{J}}_2\hat{s}_1\hat{s}_2(-1)^L\begin{Bmatrix}l_1&s_1&j_1\\ \mathcal{L}_1&\frac{1}{2}&\mathcal{J}_1\\ L&S&J\end{Bmatrix}\begin{Bmatrix}l_2&s_2&j_2\\ \mathcal{L}_2&\frac{1}{2}&\mathcal{J}_2\\ L&S&J\end{Bmatrix}\begin{Bmatrix}\frac{1}{2}&\frac{1}{2}&s_1\\ \frac{1}{2}&S&s_2\end{Bmatrix}\\ &\quad\times\langle n_1l_1\mathcal{N}_1\mathcal{L}_1L|\mathcal{N}_2\mathcal{L}_2n_2l_2L\rangle_3,\end{aligned} \tag{31}$$

where $N_i=2n_i+l_i+2\mathcal{N}_i+\mathcal{L}_i$, $i=1,2$; $\hat{j}=\sqrt{2j+1}$; and $\langle n_1l_1\mathcal{N}_1\mathcal{L}_1L|\mathcal{N}_2\mathcal{L}_2n_2l_2L\rangle_3$ is the general HO bracket for two par-

ticles with mass ratio 3 as defined, e.g., in Ref. [27]. The expression (31) can be derived by examining the action of $\mathcal{T}_{23}$ on the basis states (29). That operator changes the state $|nl(\vec{\xi}_1),\mathcal{NL}(\vec{\xi}_2),L\rangle$ to $|nl(\vec{\xi'}_1),\mathcal{NL}(\vec{\xi'}_2),L\rangle$, where $\vec{\xi'}_i, i=1,2$ are defined as $\vec{\xi}_i, i=1,2$ but with the single-nucleon indexes 2 and 3 exchanged. The primed Jacobi coordinates can be expressed as an orthogonal transformation of the unprimed ones. Consequently, the HO wave functions depending on the primed Jacobi coordinates can be expressed as an orthogonal transformation of the original HO wave functions. Elements of the transformation are the Talmi-Moshinsky HO brackets for two particles with the mass ratio d, with d determined from the orthogonal transformation of the coordinates, see, e.g., Ref. [27].

The resulting antisymmetrized states can be classified and expanded in terms of the original basis (29) as follows:

$$|NiJT\rangle = \sum \langle nlsjt;\mathcal{NL}J||NiJT\rangle|(nlsjt;\mathcal{NL}J)JT\rangle, \tag{32}$$

where $N=2n+l+2\mathcal{N}+\mathcal{L}$ and where we introduced an additional quantum number i that distinguishes states with the same set of quantum numbers N,J,T, e.g., $i=1,2,\ldots r$ with r the total number of antisymmetrized states for a given N,J,T. It can be obtained from computing the trace of the antisymmetrizer $\mathcal{X}$ [28]

$$r = \mathrm{Tr}\ \ \mathcal{X}^{NJT}. \tag{33}$$

C. Antisymmetrization for the *A*-nucleon system

The construction of a translationally-invariant antisymmetrized HO basis for four nucleons that contains an antisymmetrized three-nucleon subcluster was described in our earlier papers [19,26]. In this subsection we generalize and simplify this construction to the case of an arbitrary number of nucleons A. The starting point is a basis that contains an antisymmetrized subcluster of $A-1$ nucleons, e.g.,

$$|(N_{\mathrm{A\text{-}1}} i_{\mathrm{A\text{-}1}} J_{\mathrm{A\text{-}1}} T_{\mathrm{A\text{-}1}}; n_{\mathrm{A\text{-}1}} l_{\mathrm{A\text{-}1}} \mathcal{J}_{\mathrm{A\text{-}1}}) JT\rangle, \tag{34}$$

with the $(A-1)$-nucleon antisymmetrized state $|N_{\mathrm{A\text{-}1}} i_{\mathrm{A\text{-}1}} J_{\mathrm{A\text{-}1}} T_{\mathrm{A\text{-}1}}\rangle$, depending on the Jacobi coordinates $\vec{\xi}_1,\vec{\xi}_2,\ldots\vec{\xi}_{A-2}$ (24a)–(24e) and the state $|n_{\mathrm{A\text{-}1}} l_{\mathrm{A\text{-}1}} \mathcal{J}_{\mathrm{A\text{-}1}}\rangle$ that represents the last nucleon depending on the Jacobi coordinate $\vec{\xi}_{A-1}$. For a four nucleon system the state $|N_{\mathrm{A\text{-}1}} i_{\mathrm{A\text{-}1}} J_{\mathrm{A\text{-}1}} T_{\mathrm{A\text{-}1}}\rangle$ is identical to the state introduced in Eq. (32). The basis (34) is not antisymmetrized with respect to exchanges of the last nucleon with the others. However, due to the antisymmetry of the $A-1$ nucleon subcluster, the matrix elements of the antisymmetrizer $\mathcal{X}$ in the basis (34) simplifies dramatically, e.g.,

$$\langle\mathcal{X}\rangle = \frac{1}{A}[1-(A-1)\langle\mathcal{T}_{A,A-1}\rangle] \tag{35}$$

with $\mathcal{T}_{A,A-1}$ the transposition operator of the Ath and the $(A-1)$st nucleon. Its matrix element can be computed in a straightforward way as

$$\begin{aligned}
&\langle(N_{\mathrm{A\text{-}1\,L}} i_{\mathrm{A\text{-}1\,L}} J_{\mathrm{A\text{-}1L}} T_{\mathrm{A\text{-}1L}}; n_{\mathrm{A\text{-}1\,L}} l_{\mathrm{A\text{-}1\,L}} \mathcal{J}_{\mathrm{A\text{-}1\,L}}) JT|\mathcal{T}_{\mathrm{A,A\text{-}1}}|(N_{\mathrm{A\text{-}1\,R}} i_{\mathrm{A\text{-}1\,R}} J_{\mathrm{A\text{-}1R}} T_{\mathrm{A\text{-}1R}}; n_{\mathrm{A\text{-}1\,R}} l_{\mathrm{A\text{-}1\,R}} \mathcal{J}_{\mathrm{A\text{-}1\,R}}) JT\rangle \\
&= \delta_{N_{\mathrm{L}},N_{\mathrm{R}}} \sum \ \ \langle N_{\mathrm{A\text{-}2}} i_{\mathrm{A\text{-}2}} J_{\mathrm{A\text{-}2}} T_{\mathrm{A\text{-}2}}; n_{\mathrm{A\text{-}2\,L}} l_{\mathrm{A\text{-}2\,L}} \mathcal{J}_{\mathrm{A\text{-}2\,L}}||N_{\mathrm{A\text{-}1\,L}} i_{\mathrm{A\text{-}1\,L}} J_{\mathrm{A\text{-}1L}} T_{\mathrm{A\text{-}1L}}\rangle \\
&\quad\times\langle N_{\mathrm{A\text{-}2}} i_{\mathrm{A\text{-}2}} J_{\mathrm{A\text{-}2}} T_{\mathrm{A\text{-}2}}; n_{\mathrm{A\text{-}2\,R}} l_{\mathrm{A\text{-}2\,R}} \mathcal{J}_{\mathrm{A\text{-}2\,R}}||N_{\mathrm{A\text{-}1\,R}} i_{\mathrm{A\text{-}1\,R}} J_{\mathrm{A\text{-}1R}} T_{\mathrm{A\text{-}1R}}\rangle \hat{T}_{\mathrm{A\text{-}1L}} \hat{T}_{\mathrm{A\text{-}1R}} (-1)^{T_{\mathrm{A\text{-}1L}}+T_{\mathrm{A\text{-}1R}}+\mathcal{J}_{\mathrm{A\text{-}2\,L}}+\mathcal{J}_{\mathrm{A\text{-}2\,R}}} \\
&\quad\times\begin{Bmatrix} \frac{1}{2} & T_{\mathrm{A\text{-}2}} & T_{\mathrm{A\text{-}1R}} \\ \frac{1}{2} & T & T_{\mathrm{A\text{-}1L}} \end{Bmatrix} \hat{\mathcal{J}}_{\mathrm{A\text{-}2\,L}} \hat{\mathcal{J}}_{\mathrm{A\text{-}2\,R}} \hat{\mathcal{J}}_{\mathrm{A\text{-}1\,L}} \hat{\mathcal{J}}_{\mathrm{A\text{-}1\,R}} \hat{J}_{\mathrm{A\text{-}1L}} \hat{J}_{\mathrm{A\text{-}1R}} \hat{K}^2 \begin{Bmatrix} J_{\mathrm{A\text{-}2}} & \mathcal{J}_{\mathrm{A\text{-}2\,L}} & J_{\mathrm{A\text{-}1\,L}} \\ \mathcal{J}_{\mathrm{A\text{-}2\,R}} & K & \mathcal{J}_{\mathrm{A\text{-}1\,L}} \\ J_{\mathrm{A\text{-}1R}} & \mathcal{J}_{\mathrm{A\text{-}1\,R}} & J \end{Bmatrix} \begin{Bmatrix} l_{\mathrm{A\text{-}2\,L}} & l_{\mathrm{A\text{-}1\,R}} & K \\ \mathcal{J}_{\mathrm{A\text{-}1\,R}} & \mathcal{J}_{\mathrm{A\text{-}2\,L}} & \frac{1}{2} \end{Bmatrix} \\
&\quad\times\begin{Bmatrix} l_{\mathrm{A\text{-}2\,R}} & l_{\mathrm{A\text{-}1\,L}} & K \\ \mathcal{J}_{\mathrm{A\text{-}1\,L}} & \mathcal{J}_{\mathrm{A\text{-}2\,R}} & \frac{1}{2} \end{Bmatrix} \begin{Bmatrix} l_{\mathrm{A\text{-}1\,L}} & l_{\mathrm{A\text{-}2\,R}} & K \\ l_{\mathrm{A\text{-}1\,R}} & l_{\mathrm{A\text{-}2\,L}} & L \end{Bmatrix} \\
&\quad\times\hat{L}^2(-1)^{l_{\mathrm{A\text{-}2\,R}}+l_{\mathrm{A\text{-}1\,L}}+L}\langle n_{\mathrm{A\text{-}1\,L}} l_{\mathrm{A\text{-}1\,L}} n_{\mathrm{A\text{-}2\,L}} l_{\mathrm{A\text{-}2\,L}} L|n_{\mathrm{A\text{-}2\,R}} l_{\mathrm{A\text{-}2\,R}} n_{\mathrm{A\text{-}1\,R}} l_{\mathrm{A\text{-}1\,R}} L\rangle_{\mathrm{A(A\text{-}2)}},
\end{aligned} \tag{36}$$

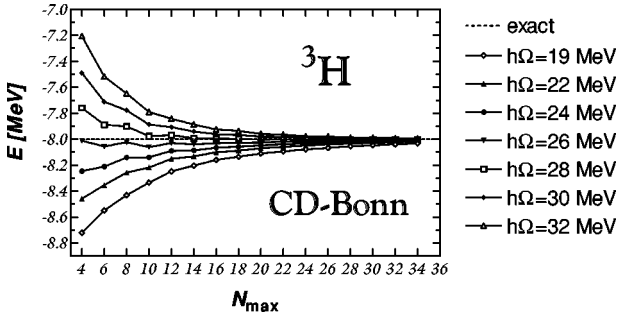

FIG. 1. The dependence of the ^{3}H ground-state energy, in MeV, on the maximal number of HO excitations allowed in the model space in the range from $N_{\max}=4$ to $N_{\max}=34$. The two-body effective interaction utilized was derived from the CD-Bonn *NN* potential. Results for $\hbar\Omega=19$, 22, 24, 26, 28, 30, and 32 MeV are presented. The dotted line represents the exact result of -8.00 MeV from a 34-channel Faddeev-equation calculation [21].

where $N_{\rm X}=N_{\rm A\text{-}1\,X}+2n_{\rm A\text{-}1\,X}+l_{\rm A\text{-}1\,X}$, X=L,R and $\langle n_{\rm A\text{-}1\,L}l_{\rm A\text{-}1\,L}n_{\rm A\text{-}2\,L}l_{\rm A\text{-}2\,L}L|n_{\rm A\text{-}2\,R}l_{\rm A\text{-}2\,R}n_{\rm A\text{-}1\,R}l_{\rm A\text{-}1\,R}L\rangle_{\rm A(A\text{-}2)}$ is the general HO bracket for two particles with mass ratio equal to $A(A-2)$. The expression (36) reduces to Eq. (19) in Ref. [19] for $A=4$. Let us stress the important property of the antisymmetrizer matrix, namely its diagonality in $N_{\rm A}\equiv N_{\rm L}=N_{\rm R}$. Consequently, we may impose a model space restriction of the type $N_{\rm A}\leqslant N_{\max}$ and still obtain all the antisymmetrized states within that model space.

The antisymmetrized states are obtained by diagonalizing the antisymmetrizer $\mathcal{X}$ (35) in the basis (34) or, more efficiently, by employing the method introduced in Ref. [29] that does not require us to compute all the matrix elements of the antisymmetrizer. In order to get the basis for the *A*-nucleon system we need to set up an iterative procedure that starts with the calculation of the three-nucleon basis (32) and procceeds to four nucleons and so on up to *A*. The resulting antisymmetrized states can be classified and expanded in terms of the original basis (34) similarly as in the three-nucleon case

$$|N_{\rm A}i_{\rm A}JT\rangle=\sum\langle N_{\rm A\text{-}1}i_{\rm A\text{-}1}J_{\rm A\text{-}1}T_{\rm A\text{-}1};n_{\rm A\text{-}1}l_{\rm A\text{-}1}\mathcal{J}_{\rm A\text{-}1}||N_{\rm A}i_{\rm A}JT\rangle \times|(N_{A-1}i_{A-1}J_{A-1}T_{A-1};n_{A-1}l_{A-1}\mathcal{J}_{A-1})JT\rangle, \tag{37}$$

where $N_{\rm A}=N_{\rm A\text{-}1}+2n_{\rm A\text{-}1}+l_{\rm A\text{-}1}$. In Eq. (37), the additional quantum number $i_{\rm A}$ distinguishes states with the same set of quantum numbers $N_{\rm A},J,T$, e.g., $i_A=1,2,\ldots r$ with r the total number of antisymmetrized states for given $N_{\rm A},J,T$. Again, it can be obtained from computing the trace of the antisymmetrizer $\mathcal{X}$

$$r=\mathrm{Tr}\,\mathcal{X}^{N_{\rm A}JT}. \tag{38}$$

We note that the expansion of the antisymmetrized basis, given in Eq. (37), is not suitable for evaluating matrix elements of two-body or three-body interactions or other operators. To facilitate calculations with such interactions and operators, different expansions of the antisymmetrized basis are needed, as described in Appendix A. Evaluation of matrix elements of one-body operators can, on the other hand, be done using the expansion (37). It is convenient to introduce one-body densities, as in the standard shell-model approach. We leave the discussion of this point to Appendix B.

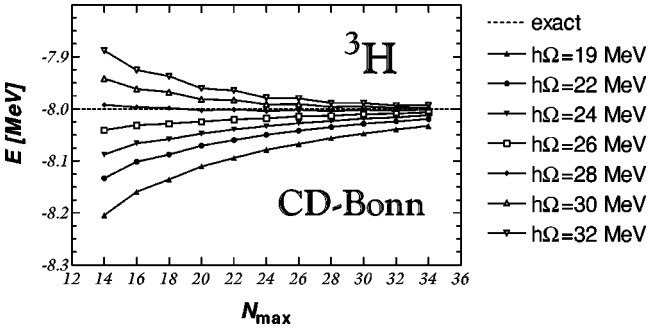

FIG. 2. The dependence of the ^{3}H ground-state energy, in MeV, on the maximal number of HO excitations allowed in the model space. The same points as in Fig. 1 for the range from $N_{\max}=14$ to $N_{\max}=34$ are presented on a larger scale.

IV. RESULTS FOR FEW-NUCLEON SYSTEMS

We have written a computer code for calculations using the formalism presented in Secs. II and III. We performed test calculations for few-nucleon systems up to $A=8$. The code reproduces results obtained using the many-fermion dynamics (MFD) shell-model code [30], when a two-body effective interaction is employed and when the model space does not require more than 9 major HO shells, i.e., the limits of the version of the MFD code we have. Due to the computational complexity of the antisymmetrization procedure we expect that the present formalism can, at the present time and in the current formulation, improve significantly on the results obtainable by the MFD code for $A\leqslant 6$ and to some extent for $A=7$ and $A=8$. Let us further remark that although the antisymmetrization is complicated it needs to be done only once for given A, N_A, J and T.

In this paper we present results for $A=3$ and $A=4$ systems, while calculations for larger A will be published sepa-

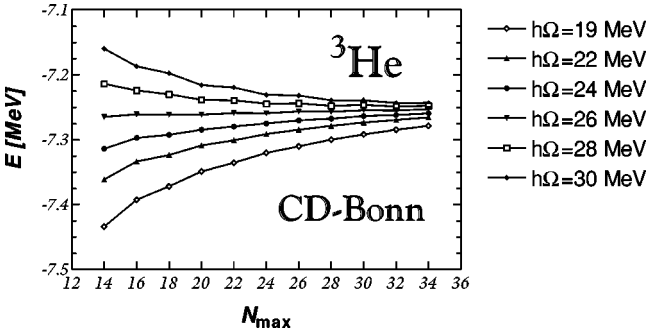

FIG. 3. The dependence of the ^{3}He ground-state energy, in MeV, on the maximal number of HO excitations allowed in the model space in the range from $N_{\max}=14$ to $N_{\max}=34$. The two-body effective interaction utilized was derived from the CD-Bonn *NN* potential. Results for $\hbar\Omega=19$, 22, 24, 26, 28, and 30 MeV are presented.

TABLE I. Results for the ground-state energies, point-proton, and point-neutron rms radii, and magnetic moments obtained for ^{3}H, ^{3}He, and ^{4}He using the CD-Bonn *NN* potential are presented. Values shown are based on the results calculated in the largest model spaces used in the present study, $N_{max}=34$ for ^{3}H, ^{3}He, and $N_{max}=16$ for ^{4}He, respectively. The errors were estimated from the dependences on the HO frequency Ω and on the model-space size characterized by N_{max}.

CD-Bonn *NN* potential	E_{gs} [MeV]	$\sqrt{\langle r_p^2\rangle}$ [fm]	$\sqrt{\langle r_n^2\rangle}$ [fm]	μ [μ_N]
^{3}H	−8.002(4)	1.608(4)	1.760(6)	2.612
^{3}He	−7.248(4)	1.802(6)	1.635(4)	−1.779
^{4}He	−26.4(2)	1.445(5)	1.445(5)	

rately at a later stage. We investigated the $A=3$ and $A=4$ systems in the framework of the present formalism in two previous papers [18] and [19], respectively. However, as the newly developed code is more efficient, we were able to extend the calculations to larger model spaces. In addition, in this paper we present results obtained using the momentum-space dependent nonlocal CD-Bonn *NN* potential [21]. There are no published results for the four-nucleon system interacting by CD-Bonn potential up to now.

We work in the isospin formalism. As the CD-Bonn *NN* potential breaks the isospin and charge symmetry we construct an isospin invariant potential for the $T=1$ two-nucleon channels by taking combinations of V_{np}, V_{pp}, and V_{nn}. For ^{3}H we take $\frac{1}{3}V_{np}+\frac{2}{3}V_{nn}$, for ^{3}He we take $\frac{1}{3}V_{np}+\frac{2}{3}V_{pp}$, while for ^{4}He we use $\frac{1}{3}V_{np}+\frac{1}{3}V_{pp}+\frac{1}{3}V_{nn}$. The Coulomb potential is added to the CD-Bonn V_{pp} potential. Similarly, for the nucleon mass we use the proton and neutron mass combinations, e.g., $m=1/A(Zm_p+Nm_n)$ with Z and N the number of protons and neutrons, respectively.

A. ^{3}H and ^{3}He

For the $A=3$ system we use the two-body effective interaction calculated as described in Sec. II D. As the effective interaction depends on the model-space size, characterized by N_{max}, and the HO frequency Ω, we investigate the dependence of observables on those two parameters. We performed calculations in the model spaces with N_{max} up to 34 for a wide range of HO frequencies Ω, e.g., $\hbar\Omega=19\ldots32$ MeV. Our ground-state results are presented in Figs. 1–3. In Fig. 1 we show the ^{3}H ground-state energy dependence on the model-space size in the range from $N_{max}=4$ to $N_{max}=34$. Different full lines connect results obtained with different HO frequencies. The dotted line represents the 34-channel Faddeev equation result −8.00 MeV [21]. It is apparent that our results converge to the Faddeev equation result as N_{max} increases. We note that the fundamental approximation used in our approach is the negligence of the three-body clusters in the expansion (13). Such clusters can give both positive and negative contribution to the ground-state energy. Our calculation is not a variational calculation. Therefore, we cannot expect a convergence from above. As seen from Fig. 1 our results converge both from above or below, with some oscillations possible, depending on the HO frequency employed. In Fig. 2 we present the same as in Fig. 1 for N_{max} in the range from 14 to 34 using an expanded energy scale. We can see that, even if a complete convergence has not been achieved for $N_{max}=34$ in the whole range of Ω used, it is possible to interpolate from the different curves to obtain the converged result. For example, the line corresponding to $\hbar\Omega=28$ MeV remains almost constant for $N_{max}>18$ at the value about −8.00 MeV. We present the interpolated results in Table I. Our ^{3}H result −8.002(4) MeV is in a good agreement with the 34-channel Faddeev calculation. We note, however, that in our calculations we used all the two-nucleon channels up to $j=6$. We should, therefore, compare with the result −8.014 MeV ob-

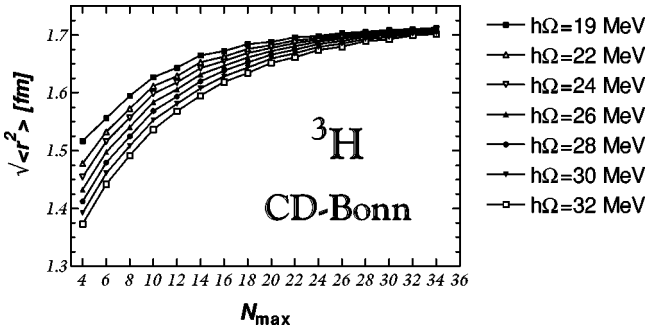

FIG. 4. The dependence of the ^{3}H point-nucleon matter radius, in fm, on the maximal number of HO excitations allowed in the model space in the range from $N_{max}=4$ to $N_{max}=34$. The two-body effective interaction utilized was derived from the CD-Bonn *NN* potential. Results for $\hbar\Omega=19$, 22, 24, 26, 28, 30, and 32 MeV are presented.

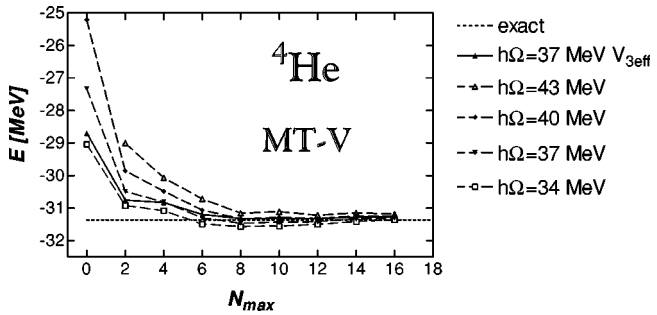

FIG. 5. The dependence of the ^{4}He ground-state energy, in MeV, on the maximal number of HO excitations allowed in the model space in the range from $N_{max}=0$ to $N_{max}=16$. The two-body (dashed lines) and three-body (full line) effective interactions utilized were derived from the Malfliet-Tjon MT-V potential. Results for $\hbar\Omega=34$, 37, 40, and 43 MeV are presented. The dotted line represents the exact result of −31.36 MeV [32].

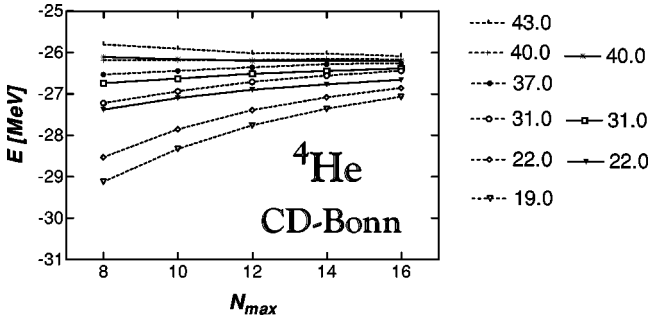

FIG. 6. The dependence of the ^{4}He ground-state energy, in MeV, on the maximal number of HO excitations allowed in the model space in the range from $N_{\max}=8$ to $N_{\max}=16$. The two-body (dotted lines) and three-body (full lines) effective interactions utilized were derived from the CD-Bonn *NN* potential. Results for $\hbar\Omega=19,\ 22,\ 31,\ 37,\ 40$, and 43 MeV are presented.

tained by Nogga *et al.* [4], where all channels with $j\leqslant 6$ were used. Consequently, it appears that we are missing about 10 keV in binding, most likely either due to imprecisions in the two-nucleon systems solutions used for construction of the effective interaction or due to the fact that we used a combination of $V_{\rm np}$, $V_{\rm pp}$, and $V_{\rm nn}$, while a combination of t-matrices was used instead in Ref. [4].

In Fig. 3, we present the same dependence for ^{3}He as in Fig. 2 for ^{3}H. Our interpolated ground-state energy result together with the error estimate is given in Table I. It should be noted that the CD-Bonn potential gives a realistic prediction for the binding energy difference of ^{3}H and ^{3}He, which is experimentally 0.764 MeV. On the other hand, the absolute value of the binding energy is underestimated compared to the experimental values, 8.482 MeV for ^{3}H and 7.718 MeV for ^{3}He, by about 400 keV. It is, however, only a half of what one gets with the local coordinate-space potentials like Nijmegen, Reid or Argonne.

The model-space size and Ω dependence of the ^{3}H point-nucleon matter rms radius is presented in Fig. 4. We observe a convergence and a saturation with the model-space size increase. In Table I we show point-proton and point-neutron rms radii for both ^{3}H and ^{3}He extrapolated from the calculations in the largest model spaces together with the error

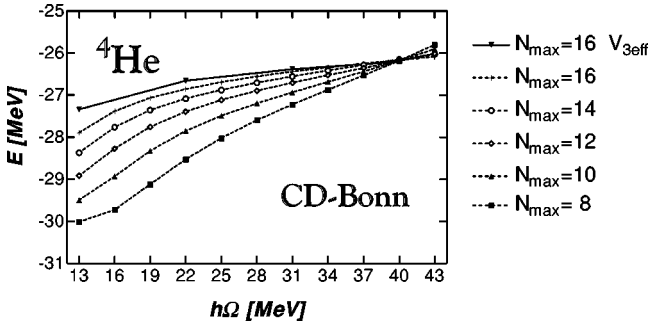

FIG. 7. The dependence of the ^{4}He ground-state energy, in MeV, on the HO energy in the range from $\hbar\Omega=13$ MeV to $\hbar\Omega=43$ MeV. The two-body (dotted lines) and three-body (full lines) effective interactions utilized were derived from the CD-Bonn *NN* potential. Results for $N_{\max}=8,\ 10,\ 12,\ 14$, and 16 are presented.

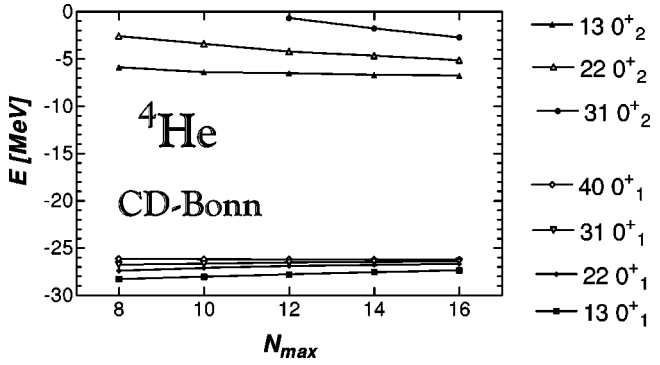

FIG. 8. The dependence of the ^{4}He ground-state and the first-excited 0^+0 state energies, in MeV, on the maximal number of HO excitations allowed in the model space in the range from $N_{\max}=8$ to $N_{\max}=16$. The three-body effective interaction utilized was derived from the CD-Bonn *NN* potential. Results for $\hbar\Omega=13,\ 22,\ 31$, and 40 MeV are presented.

estimates. In addition, the calculated magnetic moments are also presented. These can be compared to the experimental values of $+2.979\ \mu_{\rm N}$ for ^{3}H and $-2.128\ \mu_{\rm N}$ for ^{3}He. The calculated values were obtained using a one-body $M1$ operator with bare nucleon g factors.

B. ^{4}He

The calculations for ^{4}He were performed in the model spaces up to $N_{\max}=16$ in a wide range of HO frequencies Ω. This is an extension of our previous $A=4$ calculations [19], where model spaces only up to $N_{\max}=14$ were utilized and a narrower range of Ω was investigated. We performed separate calculations both with two-body effective interactions, computed as described in Sec. II D, and with three-body effective interactions, computed as discussed in Sec. II E. The three-body effective interactions were calculated for the three-nucleon channels with $J^\pi_3 T_3=\frac{1}{2}^{\pm}\frac{1}{2}$ and $J^\pi_3 T_3=\frac{3}{2}^{\pm}\frac{1}{2}$ using $N_{3\max}=32$ and $N_{3\max}=28$, respectively.

In order to test the applicability of our method to a four-nucleon system, we performed $A=4$ calculations using the

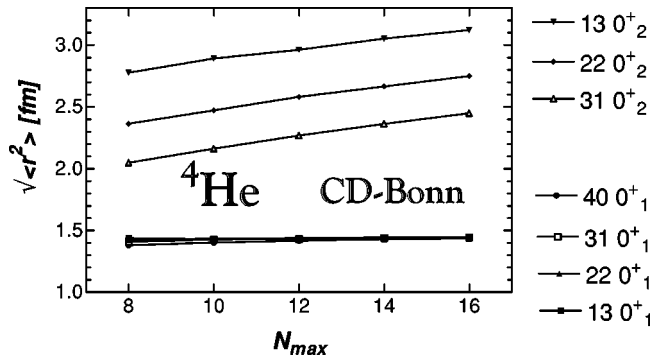

FIG. 9. The dependence of the ^{4}He ground-state and the first-excited 0^+0 state point-nucleon rms radius, in fm, on the maximal number of HO excitations allowed in the model space in the range from $N_{\max}=8$ to $N_{\max}=16$. The three-body effective interaction utilized was derived from the CD-Bonn *NN* potential. Results for $\hbar\Omega=13,\ 22,\ 31$, and 40 MeV are presented.

central Malfliet-Tjon potential MT-V [31] that is frequently used for few-body-calculation tests and for which the $A=4$ solutions have been obtained by several other methods, see, e.g., Ref. [32] and references therein. Our results are shown in Fig. 5. We present the ground-state energy dependence on the model space size in the range of $N_{\max}=0$ to $N_{\max}=16$ for different HO frequencies. Results obtained with both the two-body and the three-body effective interactions are shown, with the latter manifesting a faster convergence. We observe good convergence as the model-space size increases and, although some dependence on Ω remains even in the $N_{\max}=16$ model space, we can interpolate to obtain a ground-state energy of $-31.28(8)$ MeV, in good agreement with the exact result of -31.36 MeV, found by other methods [32]. Similarly, our point-nucleon rms radius result, 1.405(5) fm, compares well with the stochastic variational method result of 1.4087 fm [32].

Our ground-state energy results obtained with the CD-Bonn *NN* potential are presented in Figs. 6 and 7. We investigate the dependence on both $N_{\max}$ and Ω. The two figures show mostly the same points, plotted in the first case as a function of $N_{\max}$ and in the second case as a function of $\hbar\Omega$. The dotted lines connect the results obtained using the two-body effective interactions, while the full lines connect the results obtained with the three-body effective interactions. We observe a decrease of dependence on both $N_{\max}$ and $\hbar\Omega$ as the model-space size increases. In particular, the curves in Fig. 7 become more flat with increasing $N_{\max}$. Similarly as in our previous study [19], it is apparent that calculations done with the three-body effective interaction show weaker dependence on both Ω and $N_{\max}$ and demonstrate faster convergence. Due to the higher complexity of those calculations, we present results only for $\hbar\Omega=$ 13, 22, 231 and 40 MeV. As can be seen from Figs. 6 and 7, for $\hbar\Omega$ less than about 40 MeV the binding energy decreases with increasing model-space size while for larger $\hbar\Omega$ it begins to increase with increasing $N_{\max}$. Similarly as for the $A=3$ system and the $A=4$ system with MT-V potential, we are in a position to interpolate the converged ground-state energy result, though with a lower accuracy. Based on the results presented in Figs. 6 and 7, we estimate the CD-Bonn ^{4}He ground-state energy to be $-26.4(2)$ MeV. The experimental binding energy of ^{4}He is 28.296 MeV. The CD-Bonn thus underbinds ^{4}He by about 2 MeV. It is again only about a half of underbinding that one gets with, e.g., Argonne V18 with the calculated ^{4}He binding energy 24.1 MeV [33].

In our approach we obtain the ground state as well as the excited states by diagonalizing the Hamiltonian. In Figs. 8 and 9, we present the model-space-size dependence of both the ground-state and the first excited 0^+0 state energies and point-nucleon rms radii, respectively, obtained in calculations with the three-body effective interactions. Compared to the ground state, we observe a much stronger dependence by the excited-state energy and nucleon rms radius on both Ω and $N_{\max}$. The significantly different convergence rate of the ground state and of the first excited 0^+0 state manifests the different nature of the two states. A possible interpretation of this observation is that the excited 0^+0 state is associated with a radial excitation and, thus, it is more sensitive to the HO basis used in our calculations. Although we cannot extrapolate the energy or point-nucleon radius of this state, our calculations show that its excitation energy is below 21 MeV and the radius is larger than 3 fm.

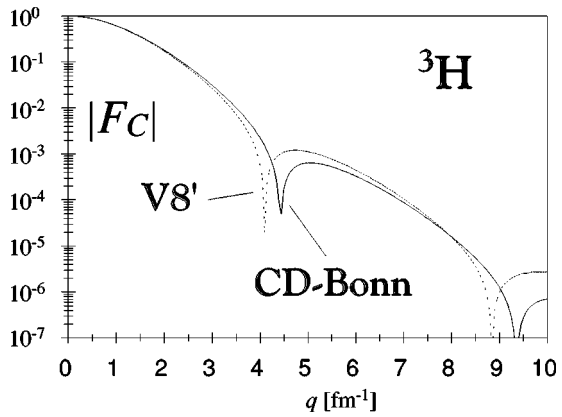

FIG. 10. The elastic EM charge form factor of ^{3}H calculated in the impulse approximation. Results obtained using the Argonne V8′ (dotted line) and CD-Bonn (full line) *NN* potentials are compared.

Our ground-state results obtained with the CD-Bonn *NN* potential are summarized in Table I.

C. Charge form factors

A sensitive test of the wave functions obtained in our calculations is the evaluation of form factors. In this subsection we compare the charge form factors obtained with the CD-Bonn wave functions and those obtained in an identical calculation with the Argonne V8′ *NN* potential defined in Ref. [10]. We note that a similar comparison was performed by Kim *et al.* in Ref. [34] for the Bonn OBEPQ and the Reid *NN* potentials. In that paper, it was found that the ^{3}H and ^{3}He form factors differ for the two *NN* potentials.

Using the formalism of Ref. [35], we calculated the charge EM form factors and ratio of charge strangeness and EM form factors in the impulse approximation. The one-body contribution to the charge operator is given by Eq. (15) in Ref. [35], e.g.,

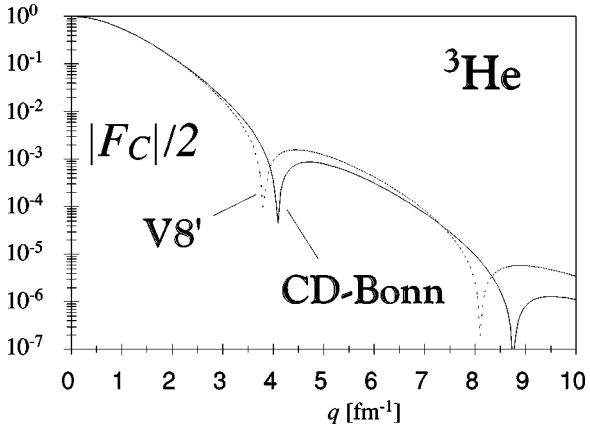

FIG. 11. The elastic EM charge form factor of ^{3}He calculated in the impulse approximation. Results obtained using the Argonne V8′ (dotted line) and CD-Bonn (full line) *NN* potentials are compared.

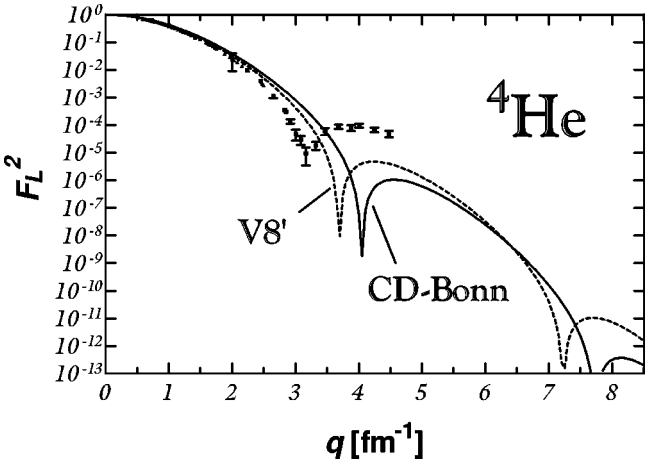

FIG. 12. The elastic EM charge form factor of ^{4}He calculated in the impulse approximation. Results obtained using the Argonne V8′ (dotted line) and CD-Bonn (full line) *NN* potentials are compared. The calculations were performed using three-body effective interaction in the model space characterized by $N_{\max}=16$ and $\hbar\Omega=22$ MeV.

$$\hat{M}^{(a)}_{00}(q)^{[1]}=\frac{1}{2\sqrt{\pi}}\sum_{k=1}^{A}\hat{O}^{(a)}_k\left\{\frac{G^{(a)}_E(\tau)}{\sqrt{1+\tau}}j_0(qr_k)+[G^{(a)}_E(\tau)-2G^{(a)}_M(\tau)]2\tau\frac{j_1(qr_k)}{qr_k}\sigma_k\cdot\mathbf{L}_k\right\}, \tag{39}$$

where $\tau=q^2/4m_N^2$, $\mathbf{L}_k$ is the kth nucleon orbital momentum, $G^{(a)}_E(\tau)$ and $G^{(a)}_M(\tau)$ are the one-body electric and magnetic form factors, respectively. The superscript (a) refers to (p) and (n) for proton and neutron EM form factor, respectively, or to (s) for the strangeness form factor. The operator $\hat{O}^{(a)}$ is equal to $(\frac{1}{2}+t_z)$ $((\frac{1}{2}-t_z))$ for $a\equiv p(a\equiv n)$ and it is equal to 1 for $a\equiv s$. We use the parametrization of the one-body form factors as discussed in Ref. [35]. We note that the one-body strangeness form factors depend on the strangeness radius ρ_s, for which we take the value $\rho_s=-2.0$ as in Ref. [35]

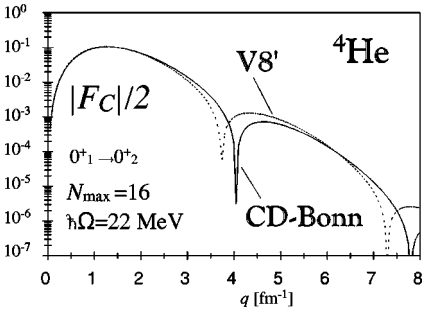

FIG. 13. The EM charge form factor of ^{4}He corresponding to the transition to the first excited 0^+0 state calculated in the impulse approximation. Results obtained using the Argonne V8′ (dotted line) and CD-Bonn (full line) *NN* potentials are compared. The calculations were performed using three-body effective interaction in the model space characterized by $N_{\max}=16$ and $\hbar\Omega=22$ MeV.

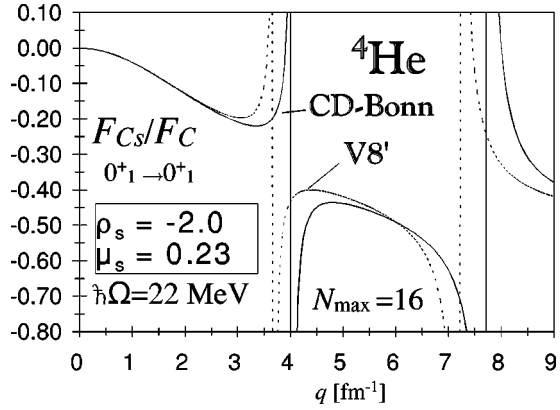

FIG. 14. The ratio of elastic strangeness and EM charge form factor of ^{4}He calculated in the impulse approximation. Results obtained using the Argonne V8′ (dotted line) and CD-Bonn (full line) *NN* potentials are compared. The calculations were performed using three-body effective interaction in the model space characterized by $N_{\max}=16$ and $\hbar\Omega=22$ MeV. Values of the strangeness radius $\rho_s=-2.0$ and the strangeness magnetic moment $\mu_s=0.23$ were employed.

and on the strangeness magnetic moment μ_s. Limits on these parameters are to be determined in the experiments at the Thomas Jefferson Accelerator Facility (TJNAF). The first strangeness magnetic-moment measurement was reported recently [36] and an experimental value $\mu_s=+0.23$, obtained with a large error. We use this value in our calculations.

The elastic EM charge form factors of ^{3}H and ^{3}He are presented in Figs. 10 and 11, respectively. We observe a large sensitivity to the choice of the *NN* potential. Let us remark that we used the wave functions obtained in the model space with $N_{\max}=34$. We investigated the dependence of the form factors on both $N_{\max}(=30,32,34)$ and $\hbar\Omega$ and found that the dependence is below the resolution of the figures. Our Argonne V8′ results compare well with those obtained using the Argonne V18 in the impulse approximation presented, e.g., in Ref. [33]. We note that the experimental position of the minima as about 3.6 fm^{-1} and 3.2 fm^{-1} for ^{3}H and ^{3}He, respectively, see Ref. [33] and the references therein.

The ^{4}He elastic EM charge form factor and the EM charge form factor corresponding to the transition to the first excited 0^+0 state are presented in Figs. 12 and 13, respectively. The three-body effective interactions were used and the $N_{\max}=16$ model spaces. For the Argonne V8′, the current results can be compared to those presented in Ref. [19] obtained using $N_{\max}=14$. We note that a second minimum appears in our calculated charge form factors in a similar position as found in the VMC calculations presented in Ref. [37]. The elastic charge form factor sensitivity to both $N_{\max}$ and $\hbar\Omega$ is weak for q below the secondary maximum but it increases for larger q. As to the inelastic form factor, there the sensitivity is significantly stronger. We believe that the form factors presented in Fig. 13 are more realistic than the inelastic ones given in Ref. [19] that we obtained using $N_{\max}=14$.

In general, for all ^{3}H, ^{3}He, and ^{4}He the CD-Bonn results

are further from the experimental data points than the results obtained using the Argonne V8′. This is in full agreement with the calculations in Ref. [34] for ^{3}H and ^{3}He. However, in order to make any conclusion about the superiority of any of the potentials, one needs to calculate the meson exchange current contributions.

Finally, in Fig. 14 we present the ratio of the ^{4}He charge strangeness and EM form factors calculated in the impulse approximation using both the Argonne V8′ and the CD-Bonn *NN* potentials. The ratio of the elastic charge form factors is particularly interesting, as it can be experimentaly obtained from the measurement of the parity-violating left-right asymmetry for scattering of polarized electrons from a ^{4}He target. Experiments of this type are now under preparation at TJNAF.

V. CONCLUSIONS

We presented a translationally invariant formulation of the no-core shell-model approach for few-nucleon systems and introduced a general method of antisymmetrization of a HO basis depending on Jacobi coordinates. The latter procedure starts with the construction of the antisymmetrized basis for three nucleons, then procceeds to four and so on. We derived an iterative algebraic formula for computing the antisymmetrized basis for A nucleons from the antisymmetrized basis for $A-1$ nucleons. In addition, we discussed how to transform the antisymmetrized states to bases containing different antisymmetrized subclusters of nucleons. The chosen approach has the advantage that the antisymmetrizer is very simple and that the dimensions of the starting basis, formed by the $A-1$ nucleon antisymmetrized subcluster and the last nucleon, are the lowest compared to bases with different subclustering.

There are two main advantages of the use of a translationally-invariant basis. First, it allows us to employ larger model spaces than in traditional shell-model calculations. Second, in addition to two-body effective interactions, three- or higher-body effective interactions as well as real three-body interactions can be utilized. The use of higher-body effective interactions reduces the dependence on the HO frequency and speeds up the convergence of our approach.

As the antisymmetrization procedure is computationally involved, the practical applicability of the formalism is limited to light nuclei. In the present formulation we expect that significant improvement over the traditional shell-model results can be achieved for $A \leqslant 6$ and to some extent for $A=7$ and $A=8$. However, different paths of antisymmetrization than that realized here can be chosen for more complex nuclei. On the other hand, there exists a sophisticated approach for antisymmetrization of hyperspherical functions depending on Jacobi coordinates developed by Barnea and Novoselsky [38]. It makes use of the orthogonal group transformations of Jacobi coordinates. That approach can be adapted for the HO functions and should lead to a more efficient antisymmetrization. Another issue is the transformation to $A-2$ plus 2 and $A-3$ plus 3 clusters as discussed in Appendix A. In principle, it can be avoided by using the reverse ordering of the Jacobi coordinates (24a)–(24e) [39]. Then, however, the computation of the one-body densities, as described in Appendix B, would become very difficult.

We applied this formalism to solve for the properties of the three- and four-nucleon systems interacting by the CD-Bonn *NN* potential in model spaces that included up to $34\hbar\Omega$ and $16\hbar\Omega$ HO excitations, respectively. For the three-nucleon system our method leads to the exact solution and our results are in agreement with the calculations by other methods. For the four-nucleon system, we first performed test calculations using the MT-V potential that confirm convergence of our method. For the calculations with the CD-Bonn potential, we were able to interpolate the ground-state energy solution from the model-space and HO-frequency dependencies. Our result with an error estimate is $-26.4(2)$ MeV. There have not been any published results so far by other methods for the $A=4$ system interacting by the CD-Bonn *NN* potential. However, we have learned of a preliminary result, -26.3 MeV, obtained by Nogga using the Faddeev-Yakubovsky equation approach [40] that is in a good agreement with our result. In addition to energies, rms radii and magnetic moments, we also compared charge form factors obtained using the CD-Bonn and Argonne V8′ *NN* potentials and found a substantial sensitivity to the choice of the potential, in agreement with results published in Ref. [34] for calculations with similar potentials.

We believe that the method discussed in this paper has the potential to solve the few-nucleon problem beyond $A=4$. The convergence can still be improved by employing four- or higher-body effective interactions in a similar fashion as we have used the three-body effective interaction. Also the antisymmetrization procedure can be made more efficient. Our method has the advantage, compared to, e.g., the GFMC method, that we solve the Schrödinger equation by diagonalization. Consequently, wave functions are obtained and excited states with identical quantum numbers as the ground state are computed. As calculations with the real three-body interactions are possible in the present formalism, we are already working to include Tucson-Melbourne or Urbana type interactions in our future studies. It would also be interesting to compare the present method with a new approach, relying also on the HO basis, in which the effective interaction is constructed by solving the Bloch-Horowitz equation [41]. Calculations are now under way for $A=5$ and $A=6$ using the present formalism.

ACKNOWLEDGMENTS

We would like to thank R. Machleidt for providing the computer code for the CD-Bonn *NN* potential. We also thank Kenji Suzuki and Nir Barnea for useful discussions. This work was supported in part by NSF Grants No. PHY96-05192 and INT98-06614. G.P.K. acknowledges the CIES for financial support while at the University of Arizona and partial support from Grant No. 391 of the Lithuanian State Science and Studies Foundation.

APPENDIX A: RECOUPLING TO BASIS CONTAINING TWO- AND THREE-BODY CLUSTERS

The A-nucleon antisymmetrized basis, obtained in Sec. III C, is given as an expansion of the basis (34), as shown in

Eq. (37). In this form, it is not, however, in general suitable for calculations with two-body or three-body interactions or other operators. In order to facilitate the calculations with two-body or three-body interactions we need to expand the antisymmetrized states $|N_{\rm A} i_{\rm A} JT\rangle$ in a HO basis consisting of antisymmetrized subclusters of $A-2$ and 2 nucleons depending on the Jacobi coordinates (25a)–(25c) or consisting of antisymmetrized subclusters of $A-3$ and 3 nucleons depending on the Jacobi coordinates (26a)–(26d), respectively.

For a calculation for an $A>3$ system with a two-body interaction, we need the following expansion matrix element:

$$\langle (N_{\rm A\text{-}2} i_{\rm A\text{-}2} J_{\rm A\text{-}2} T_{\rm A\text{-}2}; (nlsjt,\mathcal{NL})\mathcal{J})JT | N_{\rm A} i_{\rm A} JT\rangle = \sum \langle N_{\rm A\text{-}1} i_{\rm A\text{-}1} J_{\rm A\text{-}1} T_{\rm A\text{-}1}; n_{\rm A\text{-}1} l_{\rm A\text{-}1} \mathcal{J}_{\rm A\text{-}1} || N_{\rm A} i_{\rm A} JT\rangle$$

$$\times \langle N_{\rm A\text{-}2} i_{\rm A\text{-}2} J_{\rm A\text{-}2} T_{\rm A\text{-}2}; n_{\rm A\text{-}2} l_{\rm A\text{-}2} \mathcal{J}_{\rm A\text{-}2} || N_{\rm A\text{-}1} i_{\rm A\text{-}1} J_{\rm A\text{-}1} T_{\rm A\text{-}1}\rangle \hat{\mathcal{J}}_{\rm A\text{-}1} \hat{\mathcal{J}}_{\rm A\text{-}2} \hat{\mathcal{J}} \hat{J}_{\rm A\text{-}1} \hat{j} \hat{s} (-1)^{\mathcal{J}_{\rm A\text{-}2}+\mathcal{J}_{\rm A\text{-}1}+J_{\rm A\text{-}2}+J+j+\mathcal{L}+s+l_{\rm A\text{-}1}+l_{\rm A\text{-}2}} (-1)^{T_{\rm A\text{-}2}+T+1} \hat{T}_{\rm A\text{-}1} \hat{t}$$

$$\times \begin{Bmatrix} T_{\rm A\text{-}2} & \frac{1}{2} & T_{\rm A\text{-}1} \\ \frac{1}{2} & T & t \end{Bmatrix} \begin{Bmatrix} l_{\rm A\text{-}2} & \frac{1}{2} & \mathcal{J}_{\rm A\text{-}2} \\ l_{\rm A\text{-}1} & \frac{1}{2} & \mathcal{J}_{\rm A\text{-}1} \\ L & s & \mathcal{J} \end{Bmatrix} \begin{Bmatrix} J_{\rm A\text{-}2} & \mathcal{J}_{\rm A\text{-}2} & J_{\rm A\text{-}1} \\ \mathcal{J}_{\rm A\text{-}1} & J & \mathcal{J} \end{Bmatrix} \begin{Bmatrix} s & l & j \\ \mathcal{L} & \mathcal{J} & L \end{Bmatrix} \hat{L}^2 \langle nl\mathcal{NL}L | n_{\rm A\text{-}1} l_{\rm A\text{-}1} n_{\rm A\text{-}2} l_{\rm A\text{-}2} L\rangle_{\rm A/(A\text{-}2)}, \tag{A1}$$

where we used an orthogonal transformation of the Jacobi coordinates $\vec{\xi}_{A-2}, \vec{\xi}_{A-1}$ and $\vec{\eta}_{A-2}, \vec{\eta}_{A-1}$. In the state $|(N_{\rm A\text{-}2} i_{\rm A\text{-}2} J_{\rm A\text{-}2} T_{\rm A\text{-}2}; (nlsjt,\mathcal{NL})\mathcal{J})JT\rangle$, the antisymmetrized subcluster $|N_{\rm A\text{-}2} i_{\rm A\text{-}2} J_{\rm A\text{-}2} T_{\rm A\text{-}2}\rangle$ depends on the Jacobi coordinates $\vec{\xi}_1, \vec{\xi}_2, \ldots \vec{\xi}_{A-3}$. The two-nucleon channel state $|nlsjt\rangle$ depends on the Jacobi coordinate $\vec{\eta}_{A-1}$ and the HO state $|\mathcal{NL}\rangle$ that describes the relative motion of the two subclusters is associated with the Jacobi coordinate $\vec{\eta}_{A-2}$, given in Eq. (25).

When this expansion of $|N_{\rm A} i_{\rm A} JT\rangle$ is used a matrix element of a two-body interaction in the basis $|N_{\rm A} i_{\rm A} JT\rangle$ can be evaluated in a simple manner, e.g.,

$$\left\langle \sum_{i<j=1}^{A} V_{ij} \right\rangle = \frac{1}{2} A(A-1) \langle V(\sqrt{2}\,\vec{\eta}_{A-1})\rangle, \tag{A2}$$

and the matrix element on the right-hand side is diagonal in all quantum numbers of the state $|(N_{\rm A\text{-}2} i_{\rm A\text{-}2} J_{\rm A\text{-}2} T_{\rm A\text{-}2}; (nlsjt,\mathcal{NL})\mathcal{J})JT\rangle$ except n,l for an isospin invariant interaction.

Similarly, for a calculation for an $A>5$ system with a three-body interaction, we need the following expansion matrix element:

$$\langle (N_{\rm A\text{-}3} i_{\rm A\text{-}3} J_{\rm A\text{-}3} T_{\rm A\text{-}3}; (N_3 i_3 J_3 T_3, \mathcal{NL})\mathcal{J})JT | N_{\rm A} i_{\rm A} JT\rangle = \sum \langle N_{\rm A\text{-}2} i_{\rm A\text{-}2} J_{\rm A\text{-}2} T_{\rm A\text{-}2}; (nlsjt,\mathcal{N}'\mathcal{L}')\mathcal{J}' || N_{\rm A} i_{\rm A} JT\rangle$$

$$\times \langle N_{\rm A\text{-}3} i_{\rm A\text{-}3} J_{\rm A\text{-}3} T_{\rm A\text{-}3}; n_{\rm A\text{-}3} l_{\rm A\text{-}3} \mathcal{J}_{\rm A\text{-}3} || N_{\rm A\text{-}2} i_{\rm A\text{-}2} J_{\rm A\text{-}2} T_{\rm A\text{-}2}\rangle \langle nlsjt; n'_{\rm A\text{-}3} l'_{\rm A\text{-}3} \mathcal{J}'_{\rm A\text{-}3} || N_3 i_3 J_3 T_3\rangle \hat{\mathcal{J}}_{\rm A\text{-}3} \hat{\mathcal{J}}'_{\rm A\text{-}3} \hat{\mathcal{J}} \hat{\mathcal{J}}' \hat{J}_{\rm A\text{-}2} \hat{J}_3$$

$$\times (-1)^{\mathcal{J}'+J_{\rm A\text{-}3}+J+j+l_{\rm A\text{-}3}+1/2} (-1)^{T_{\rm A\text{-}3}+T_3+T} \hat{T}_{\rm A\text{-}2} \hat{T}_3 \begin{Bmatrix} T_{\rm A\text{-}3} & \frac{1}{2} & T_{\rm A\text{-}2} \\ t & T & T_3 \end{Bmatrix} \begin{Bmatrix} J_{\rm A\text{-}3} & J & \mathcal{J} \\ \mathcal{J}' & \mathcal{J}_{\rm A\text{-}3} & J_{\rm A\text{-}2} \end{Bmatrix} \hat{K}^2 (-1)^K \begin{Bmatrix} \mathcal{J}'_{\rm A\text{-}3} & J_3 & j \\ l'_{\rm A\text{-}3} & \mathcal{L} & L \\ \frac{1}{2} & \mathcal{J} & K \end{Bmatrix}$$

$$\times \begin{Bmatrix} \mathcal{J}' & l_{\rm A\text{-}3} & K \\ \frac{1}{2} & \mathcal{J} & \mathcal{J}_{\rm A\text{-}3} \end{Bmatrix} \begin{Bmatrix} \mathcal{J}' & l_{\rm A\text{-}3} & K \\ L & j & \mathcal{L}' \end{Bmatrix} \hat{L}^2 (-1)^L \langle n'_{\rm A\text{-}3} l'_{\rm A\text{-}3} \mathcal{NL} L | n_{\rm A\text{-}3} l_{\rm A\text{-}3} \mathcal{N}' \mathcal{L}' L\rangle_{2({\rm A\text{-}3})/{\rm A}}. \tag{A3}$$

Here we used an orthogonal transformation of the Jacobi coordinates $\vec{\xi}_{A-3}, \vec{\eta}_{A-2}$ and $\vec{\vartheta}_{A-3}, \vec{\vartheta}_{A-2}$ given in Eqs. (25a)–(26d). In the state $|(N_{\rm A\text{-}3} i_{\rm A\text{-}3} J_{\rm A\text{-}3} T_{\rm A\text{-}3}; (N_3 i_3 J_3 T_3, \mathcal{NL})\mathcal{J})JT\rangle$, the antisymmetrized subcluster $|N_{\rm A\text{-}3} i_{\rm A\text{-}3} J_{\rm A\text{-}3} T_{\rm A\text{-}3}\rangle$ depends on the Jacobi coordinates $\vec{\xi}_1, \vec{\xi}_2, \ldots \vec{\xi}_{A-4}$. The three-nucleon antisymmetrized subcluster $|N_3 i_3 J_3 T_3\rangle$ depends on the Jacobi coordinates $\vec{\vartheta}_{A-2}, \vec{\eta}_{A-1}$ and the HO state $|\mathcal{NL}\rangle$ that describes the relative motion of the two subclusters is associated with the Jacobi coordinate $\vec{\vartheta}_{A-3}$, given in Eq. (26).

When this expansion of $|N_{\rm A} i_{\rm A} JT\rangle$ is used a matrix element of a three-body interaction in the basis $|N_{\rm A} i_{\rm A} JT\rangle$ can be evaluated in a straightforward way, e.g.,

$$\left\langle \sum_{i<j<k=1}^{A} V_{ijk} \right\rangle = \frac{1}{6} A(A-1)(A-2) \langle V(\vec{\vartheta}_{A-2}, \vec{\eta}_{A-1}) \rangle, \tag{A4}$$

and the matrix element on the right-hand side is diagonal in all quantum numbers of the state $|(N_{\rm A\text{-}3} i_{\rm A\text{-}3} J_{\rm A\text{-}3} T_{\rm A\text{-}3}; (N_3 i_3 J_3 T_3, \mathcal{NL}) \mathcal{J}) JT\rangle$, except N_3 and i_3, for an isospin invariant interaction.

APPENDIX B: ONE-BODY DENSITIES

In the formalism of the translationally-invariant shell model, one can introduce one- or higher-body densities, as in the standard shell-model formulation. Let us consider a general one-body operator, e.g.,

$$\hat{O}^{(k\tau)} = \sum_{i=1}^{A} \hat{O}^{(k\tau)}(\vec{r}_i - \vec{R}, \vec{\sigma}_i, \vec{\tau}_i). \tag{B1}$$

Its matrix element between antisymmetrized states depending on the Jacobi coordinates (24a)–(24e) can be written schematically as

$$\langle \hat{O}^{(k\tau)} \rangle = A \left\langle \hat{O}^{(k\tau)} \left(- \sqrt{\frac{A-1}{A}} \vec{\xi}_{A-1}, \vec{\sigma}_A, \vec{\tau}_A \right) \right\rangle. \tag{B2}$$

In a more detailed form, we can express a reduced matrix element between two eigenstates of a Hamiltonain corresponding to A-nucleon system as

$$\langle A; E J^{\pi} T || \hat{O}^{(k\tau)} || A; E' J'^{\pi'} T' \rangle = \sum \langle A; E J^{\pi} T | (N_{\rm A\text{-}1} i_{\rm A\text{-}1} J_{\rm A\text{-}1} T_{\rm A\text{-}1}; n_{\rm A\text{-}1} l_{\rm A\text{-}1} \mathcal{J}_{\rm A\text{-}1}) JT \rangle$$

$$\times \langle (N_{\rm A\text{-}1} i_{\rm A\text{-}1} J_{\rm A\text{-}1} T_{\rm A\text{-}1}; n'_{\rm A\text{-}1} l'_{\rm A\text{-}1} \mathcal{J}'_{\rm A\text{-}1}) J' T' | A; E' J'^{\pi'} T' \rangle \hat{J} \hat{J}' (-1)^{J_{\rm A\text{-}1} + K + J + \mathcal{J}'_{\rm A\text{-}1}} \begin{Bmatrix} J_{\rm A\text{-}1} & \mathcal{J}_{\rm A\text{-}1} & J' \\ K & J & \mathcal{J}_{\rm A\text{-}1} \end{Bmatrix} \hat{T} \hat{T}' (-1)^{T_{\rm A\text{-}1} + \tau + T + 1/2}$$

$$\times \begin{Bmatrix} T_{\rm A\text{-}1} & \frac{1}{2} & T' \\ \tau & T & \frac{1}{2} \end{Bmatrix} \left\langle n_{\rm A\text{-}1} l_{\rm A\text{-}1} \mathcal{J}_{\rm A\text{-}1} \left| \left| \left| A \hat{O}^{(k\tau)} \left(- \sqrt{\frac{A-1}{A}} \vec{\xi}_{A-1}, \vec{\sigma}_A, \vec{\tau}_A \right) \right| \right| \right| n'_{\rm A\text{-}1} l'_{\rm A\text{-}1} \mathcal{J}'_{\rm A\text{-}1} \right\rangle, \tag{B3}$$

where we used expansions of the eigenstates in the basis (37). Apparently, the matrix element (B3) factorizes into products of one-body reduced matrix elements and one-body densities.

One can introduce two- or higher-body densities in a similar way.

[1] L.D. Faddeev, Zh. Éksp. Teor. Fiz. **39**, 1459 (1960) [Sov. Phys. JETP **12**, 1014 (1961)].

[2] C.R. Chen, G.L. Payne, J.L. Friar, and B.F. Gibson, Phys. Rev. C **31**, 2266 (1985).

[3] J.L. Friar, G.L. Payne, V.G.J. Stoks, and J.J. de Swart, Phys. Lett. B **311**, 4 (1993).

[4] A. Nogga, D. Hüber, H. Kamada, and W. Glöckle, Phys. Lett. B **409**, 19 (1997).

[5] O. A. Yakubovsky, Yad. Fiz. **5**, 1312 (1966) [Sov. J. Nucl. Phys. **5**, 937 (1966)].

[6] W. Glöckle and H. Kamada, Phys. Rev. Lett. **71**, 971 (1993).

[7] F. Ciesielski and J. Carbonell, Phys. Rev. C **58**, 58 (1998); F. Ciesielski, J. Carbonell, and C. Gignoux, Nucl. Phys. **A631**, 653c (1998).

[8] M. Viviani, A. Kievsky, and S. Rosati, Few-Body Syst. **18**, 25 (1995).

[9] N. Barnea, W. Leidemann, and G. Orlandini, Nucl. Phys. **A650**, 427 (1999).

[10] B. S. Pudliner, V. R. Pandharipande, J. Carlson, S. C. Pieper, and R. B. Wiringa, Phys. Rev. C **56**, 1720 (1997); R. B. Wiringa, Nucl. Phys. **A631**, 70c (1998).

[11] R. F. Bishop, M. F. Flynn, M. C. Boscá, E. Buendía, and R. Guardiola, Phys. Rev. C **42**, 1341 (1990).

[12] J. H. Heisenberg and B. Mihaila, Phys. Rev. C **59**, 1440 (1999).

[13] D. C. Zheng, J. P. Vary, and B. R. Barrett, Phys. Rev. C **50**, 2841 (1994); D. C. Zheng, B. R. Barrett, J. P. Vary, W. C. Haxton, and C. L. Song, *ibid.* **52**, 2488 (1995).

[14] P. Navrátil and B. R. Barrett, Phys. Rev. C **54**, 2986 (1996); **57**, 3119 (1998).
[15] P. Kramer and M. Moshinsky, Nucl. Phys. **82**, 241 (1966).
[16] T. S. Makharadz and T. Ya. Mikhelashvili, Yad. Fiz. **13**, 981 (1971) [Sov. J. Nucl. Phys. **13**, 564 (1971)]; L. Majling, J. Řízek, Z. Pluhař, and Y. F. Smirnov, J. Phys. G **2**, 357 (1976).
[17] G. P. Kamuntavičius, Lith. Phys. Collect. **28**, 135 (1988); A. Deveikis and G. P. Kamuntavičius, Lith. Phys. J. **36**, 83 (1996); **37**, 371 (1997).
[18] P. Navrátil and B. R. Barrett, Phys. Rev. C **57**, 562 (1998).
[19] P. Navrátil and B. R. Barrett, Phys. Rev. C **59**, 1906 (1999).
[20] K. Suzuki, Prog. Theor. Phys. **68**, 1999 (1982); K. Suzuki and R. Okamoto, *ibid.* **92**, 1045 (1994).
[21] R. Machleidt, F. Sammarruca, and Y. Song, Phys. Rev. C **53**, 1483 (1996).
[22] V. G. J. Stoks, R. A. M. Klomp, C. P. F. Terheggen, and J. J. de Swart, Phys. Rev. C **49**, 2950 (1994).
[23] K. Suzuki and S.Y. Lee, Prog. Theor. Phys. **64**, 2091 (1980).
[24] K. Suzuki, Prog. Theor. Phys. **68**, 246 (1982); K. Suzuki and R. Okamoto, *ibid.* **70**, 439 (1983).
[25] J. Da Providencia and C. M. Shakin, Ann. Phys. (N.Y.) **30**, 95 (1964).
[26] P. Navrátil, B. R. Barrett, and W. Glöckle, Phys. Rev. C **59**, 611 (1999).
[27] L. Trlifaj, Phys. Rev. C **5**, 1534 (1972).
[28] G. P. Kamuntavičius, Fiz. Elem. Chastits At. Yadra **20**, 261 (1989) [Sov. J. Part. Nucl. **20**, 109 (1989)].
[29] A. Deveikis and G. P. Kamuntavičius, Lith. Phys. J. **35**, 14 (1995).
[30] J. P. Vary and D. C. Zheng, ''The Many-Fermion-Dynamics Shell-Model Code,'' Iowa State University, 1994 (unpublished).
[31] R. A. Malfliet and J. A. Tjon, Nucl. Phys. **A127**, 161 (1969).
[32] H. Kamada and W. Glöckle, Nucl. Phys. **A548**, 205 (1992); K. Varga and Y. Suzuki, Phys. Rev. C **52**, 2885 (1995).
[33] J. Carlson and R. Schiavilla, Rev. Mod. Phys. **70**, 743 (1998).
[34] Kr. T. Kim, Y. E. Kim, D. J. Klepacki, R. A. Brandenburg, E. P. Harper, and R. Machleidt, Phys. Rev. C **38**, 2366 (1988).
[35] M. J. Musolf, R. Schiavilla, and T. W. Donnelly, Phys. Rev. C **50**, 2173 (1994).
[36] B. Mueller *et al.*, Phys. Rev. Lett. **78**, 3824 (1997).
[37] R. Schiavilla, V. R. Pandharipande, and D. O. Riska, Phys. Rev. C **41**, 309 (1990).
[38] N. Barnea and A. Novoselsky, Ann. Phys. (N.Y.) **256**, 192 (1997).
[39] N. Barnea (private communication).
[40] A. Nogga (private communication).
[41] W. C. Haxton and C.-L. Song, E-print archive No. nucl-th/9906082.